Aging and Disease
www.aginganddisease.org
Volume 3, Number 2; 141-155, April 2012

Original article

Amyloid Deposition and Advanced Age Fails to Induce Alzheimer's Type Progression in a Double Knock-In Mouse Model

Gauri H. Malthankar-Phatak[1], Yin-Guo Lin[1], Nicholas Giovannone[1], Robert Siman[1,2,*]

[1]Department of Neurosurgery, University of Pennsylvania School of Medicine, and [2]Center for Brain Injury and Repair, University of Pennsylvania, Philadelphia, PA, USA

[Received July 15, 2011; Revised July 25, 2011; Accepted July 25, 2011]

ABSTRACT: It has been challenging to develop transgenic and gene-targeted mouse models that recapitulate all of the neuropathological features of Alzheimer's disease (AD). For example, in the APP/PS-1 double knock-in mutant mouse (DKI), frank neurodegeneration is not observed at middle age and synapse loss is pronounced only within amyloid plaques. Here, we investigated whether continued amyloid deposition and advanced age of 24-27 months lead to loss of neurons and synapses, tau hyperphosphorylation, and other pathological features of AD. We focused on the perforant pathway projection from entorhinal cortex to hippocampal dentate gyrus, since it is preferentially impacted by plaques, tangles, and neuronal loss early in the course of AD. Compared with wild type controls matched for age and gender, expression of neither reelin nor NeuN was altered in the entorhinal layer 2 neurons of origin. Retrograde labeling of the perforant pathway with Fluorogold indicated no cell loss, axonal atrophy, or nerve terminal degeneration. The lack of neuronal loss or atrophy was confirmed by volumetric analysis of the ventral dentate gyrus and immunostaining for a synaptic marker. We also searched for other hallmarks of AD neuropathology by labeling for hyperphosphorylated pre-tangle tau, accumulation of cathepsin D-containing autolysosomes, and cyclin A-positive neurons aberrantly re-entering the cell cycle. None of these AD pathologies were observed in the entorhinal cortex, dentate gyrus, or any other forebrain region. Our results indicate that the DKI mouse does not show appreciable Alzheimer-type disease progression, even at advanced age and in the phase of over 18 months of robust cerebral amyloid deposition. The insufficiency of amyloid deposition to induce other AD-type neuropathologies and neurodegeneration in the aging mouse brain suggests an important role for tauopathy or other factors for triggering the pathogenesis of AD.

Key words: Amyloid; aging; neuronal degeneration; Alzheimer's disease; tau; cathepsin D

Major challenges in Alzheimer's disease (AD) research have been to develop small animal models reproducing the full neuropathological and neurodegenerative spectrum of the disease, and to apply these models for delineating critical steps in disease pathogenesis. The hallmark aging- and region-dependent amyloid β deposition and its attendant neuritic dystrophy and reactive gliosis are captured in a number of mouse lines transgenic for familial AD-causing mutations in the genes for amyloid precursor protein (*APP*), presenilin-1 (*PS-1*), or bitransgenics expressing both mutant *APP* and *PS-1* (1-7). However, none of these mouse models are reported to accumulate neurofibrillary tangles containing hyperphosphorylated, aggregated tau, or exhibit robust neurodegeneration and synapse loss across the many brain regions susceptible in AD (8). The inability of mutant APP and PS-1 to induce widespread and profound AD-type neuropathology and neurodegeneration in the mouse without other genetic modifications is not simply a limitation of transgenesis.

***Correspondence should be addressed to:** Dr. Robert Siman, Department of Neurosurgery, Philadelphia, PA 19104, USA. Email – siman@mail.med.upenn.edu
ISSN: 2152-5250

In the APP/PS-1 double knock-in mouse model (DKI) of Alzheimer's disease (AD), which does not overexpress mutant APP and PS-1, frank neurodegeneration and tau pathology are not observed out to 14 months of age and synapse loss is pronounced only within amyloid plaques (9).

The perforant pathway projection arises from entorhinal cortex layer II neurons and terminates in the molecular layer of hippocampal dentate gyrus, and plays a vital role in certain forms of long-term memory (10, 11). The pathway develops neurofibrillary tangles in the earliest pathological stages of AD (12), and shows substantial neuronal loss that is coincident with initial clinical signs of mild cognitive impairment (13) and that progresses along with the cognitive decline, until more than 90% of the pathway has degenerated (14). Unfortunately, neither APP or PS-1 transgenic mice nor the DKI model of AD have shown robust evidence for degenerative changes or neurofibrillary pathology in this entorhino-hippocampal projection, and additional genetic manipulations are required to impact the perforant pathway, such as deletion of the CD45 gene (15), reduction of reelin expression (16), or overexpression of mutant forms of tau linked to another neurodegenerative disease, frontotemporal lobar dementia (6, 17, 18). Additional pathological features of vulnerable brain regions in AD, including aberrant neuronal reentry into the cell cycle and hyperaccumulation of lysosomes and lysosome-associated autophagic vacuoles (19, 20) have not been described for the perforant pathway in mouse models of AD.

An important caveat to the incomplete AD-type neuropathology with APP and PS-1 transgenes or knock-in mutations is that aging is the biggest risk factor for AD, but few studies have examined amyloid-depositing APP and PS-1 mutant mice beyond 18 months of age for loss of neurons and synapses, tauopathy, or other neuropathological features of AD. Here, our objective was to investigate in the APP/PS-1 double knock-in mutant mouse whether advanced age of 24-27 months could couple with long-term and extensive cerebral amyloid deposition to initiate AD-type disease progression in the perforant pathway. We thoroughly evaluated neuronal survival and atrophy in the entorhino-dentate projection using cell- and compartment type-specific markers and retrograde tracing methods, and searched for other characteristics of AD pathology such as hyperphosphorylated pre-tangle tau, increased accumulation of lysosomes, and aberrant neuronal reentry into the cell cycle.

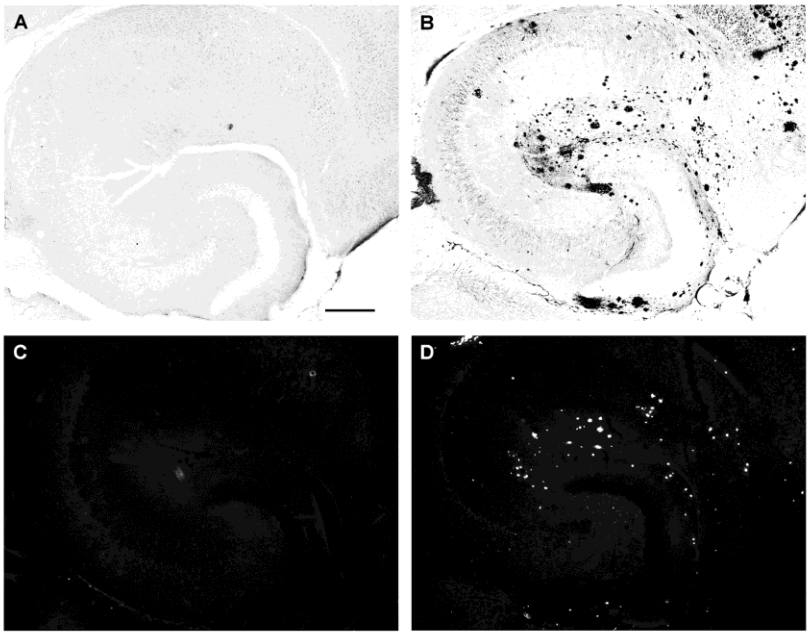

Figure 1. Amyloid plaque burden in the middle and outer molecular layers of the dentate gyrus and the deep entorhinal cortex of the DKI mouse. Amyloid β labeling by an immunoperoxidase method using AB1153 reveals an extensive amyloid burden in the DKI (B) but not the wild type (A) mouse at 24-27 months of age. Thioflavin-S staining confirms the presence of core-containing plaques in the DKI (D) but not wild type (C) mouse brain. Scale bar = 500 μm.

MATERIALS AND METHODS

Gene-targeted DKI mouse line

The APP/PS-1 double knock-in mutant mouse line was created using gene targeting in embryonic stem cells, and has been described and characterized extensively elsewhere (21-25). The mouse *APP* gene carries the Swedish double point mutation at codons 670-671, and the three variant codons within the Aβ domain have been changed from the mouse to the human sequence. The mouse *PS-1* gene carries the familial AD-linked P264L point mutation. The DKI mouse line is homozygous for the two mutant alleles for both genes. The DKI and wild type mice used in the present study were all of the CD-1 outbred strain, and were bred and aged in a pathogen-free facility at the University of Pennsylvania. Mice were given free access to food and water, and maintained under veterinary supervision in strict compliance with all standards for animal care and investigation established in the "Guide For The Care And Use Of Laboratory Animals" (National Academy Press ISBN# 0-309-05377-3). Both male and female mice 24-27 months of age were used for all studies. No differences were observed between the responses of males and females to the APP and PS-1 knock-in mutations, or any of the markers tested, and so data for the two genders were pooled.

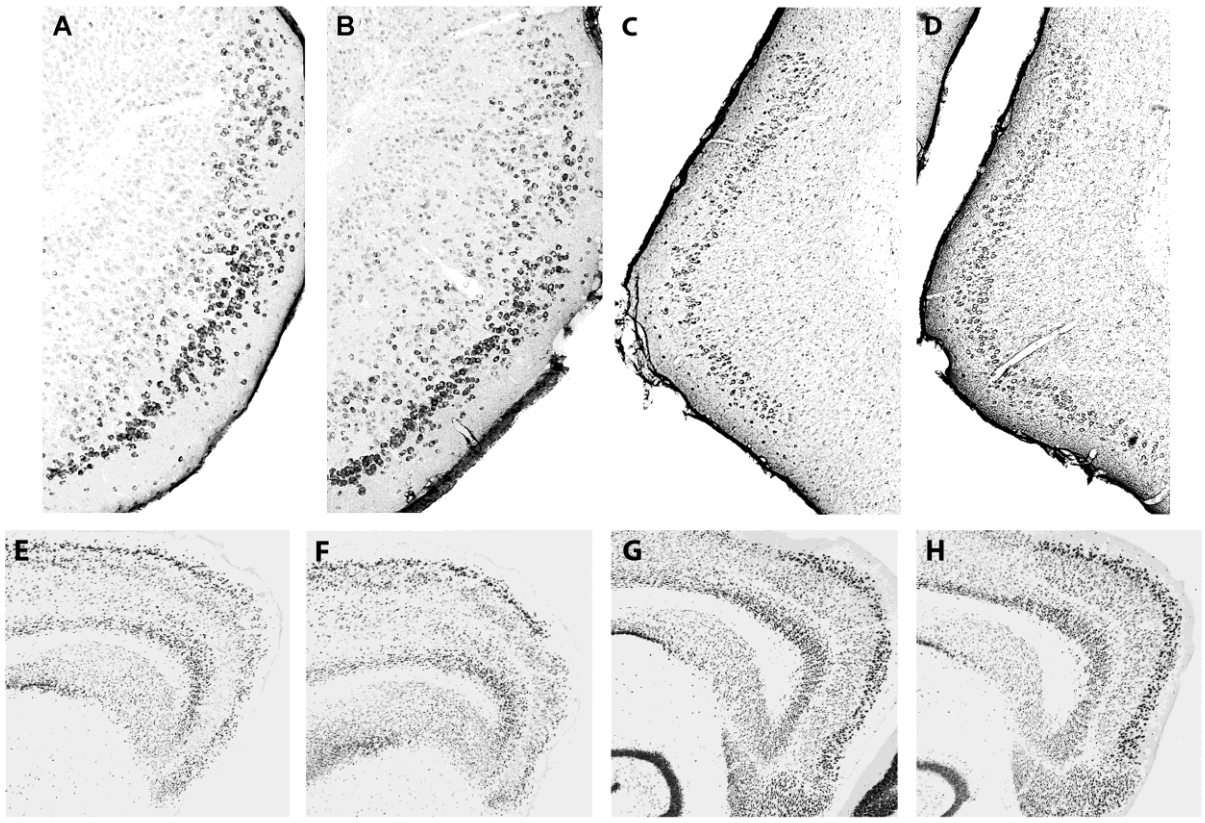

Figure 2. Absence of neuronal loss in the perforant pathway projection with advanced age and amyloid deposition. (A-D) Reelin immunostaining; (E-H) NeuN immunostaining. Neither the density of reelin-immunopositive neurons nor the reelin expression level are altered appreciably at 24-27 months of age in either the ventral or dorsal aspects of entorhinal cortex layer II in DKI mice (B, D) as compared to wild type control mice (A,C respectively); Similarly, NeuN labeling of neurons in the ventral (E,F) and dorsal (G,H) aspects of entorhinal cortex is indistinguishable between aged DKI mice (F, H) and aged wild type controls (E,G). Scale bar = 500 μm.

Immunocytochemistry and morphometry

Mice were anesthetized deeply with an overdose of pentobarbital and perfused transcardially with ice cold 0.1M sodium phosphate buffer at pH 7.4 (PB), followed by ice cold freshly prepared 4% paraformaldehyde in PB. Brains were carefully dissected, post-fixed for 4 hours at 4°C, cryoprotected in 20% sucrose in PB overnight, blocked and frozen at -40°C using dry ice in 2-methylbutane, and stored at -80°C. Horizontal sections 40 μm thick were prepared with a sliding microtome and collected sequentially into ten series, with each starting from the ventral-most edge of dentate gyrus and extending dorsally to the top of the hippocampus. The total number of sections between these anatomical boundaries did not differ as a function of APP and PS-1 genotype.

One series of at least 8 sections from each mouse was immunostained by an indirect immunoperoxidase method for amyloid Aβ (rabbit antibody 1153 at 1/10,000 dilution; (25, 26)), reelin, which is expressed at high levels in neurons of origin for the perforant pathway into adulthood (mouse antibody at 1/20,000 dilution, Millipore, Bellerica, MA; (27)), NeuN, a marker for neuron specific nuclear protein (mouse antibody at 1/30,000 dilution, Millipore, Bellerica, MA; (28)), MC1 monoclonal antibody to tau, which labels a pathological tau conformer of pre-tangles (kindly provided by Dr. Peter Davies; 1/10 dilution of hybridoma supernatant; (29)), cyclin A, a marker for cell cycle (rabbit antibody at 1/20,000 dilution, Abcam, Cambridge, MA; (30)), or cathepsin D, a marker for lysosomes and related autophagic vacuoles (rabbit antibody kindly provided by Dr. Ralph Nixon and used at 1/10,000 dilution; (31)). For immunoperoxidase staining, sections were rinsed in 20 mM Tris-HCl + 150 mM NaCl, (pH 7.4; TBS) then permeabilized and pre-blocked for 1 hour at room temperature in TBS containing 0.05% Triton X-100 + 3% normal serum from the same species as the secondary antibody. Sections were incubated in primary antibody overnight at 4°C, and then were washed three times in TBS. Next, sections were incubated with species-specific biotinylated secondary antibodies (Vector Laboratories, Burlingame, CA; 1/500 – 1/1000 dilution) for 1 hour at room temperature, washed three times in TBS, and then incubated for 1 hour at room temperature in a pre-formed avidin-biotin-horseradish peroxidase complex (prepared from the Vectastain ABC Elite kit) prepared in TBS + 0.5% bovine serum albumin and used at 1/3 the recommended strength. Following four washes in TBS, an insoluble peroxidase reaction product was formed using diaminobenzidine + H_2O_2 as chromagen. Stained sections were washed in TBS, mounted onto gelatin-coated slides, dehydrated, delipidated and coverslipped using Permount. Some sections were counterstained for fibrillar amyloid deposits using thioflavin S at 0.1%. Photomicrographs were captured under brightfield and Nomarski illumination on a Nikon Eclipse E600 microscope outfitted with a Nikon DXM-1200 camera. Images of the sections stained with thioflavin S were captured using a cooled CCD monochromatic camera and processed with NIS Elements software.

For immunofluorescence double labeling of synapses and amyloid deposits, slide-mounted sections were treated with autofluorescence quencher (Chemicon, Bellerica, MA) for 1.5 minutes, then permeabilized and pre-blocked with TBS containing 0.05% Triton X-100 and 3% normal goat serum for 1 hour at room temperature. Sections were incubated in antibodies to synaptophysin (rabbit antibody at 1/3000 dilution, Millipore, Bellerica, MA) and amyloid β (mouse antibody 6E10 at 1/1000 dilution, Invitrogen, Carlsbad, CA) overnight at 4°C, then washed three times in TBS. Next, the sections were treated for 1 hour at room temperature in the dark with goat anti-rabbit and anti-mouse secondary antibodies conjugated to AlexaFluor-488 and -568, respectively (Molecular Probes, Carlsbad, CA; 1/500 dilution each). Sections were washed three times in TBS, then coverslipped using Vectashield with DAPI (Vector Laboratories) and stored in the dark at 4°C. Photomicrographic images were captured in 8-12 z-steps of 1 μm using a motorized stage. The z-stacks were deconvolved using the autoquant algorithm of NIS-Elements and saved as the maximum intensity projection two-dimensional images compiled from digitally sectioned z-planes. Each experiment labeled and analyzed sections derived from both control and treated groups to ensure internal experimental consistency. All images for a given immunostain were taken using the same exposure time, deconvolved using equivalent settings, and prepared for publication using equivalent processing methods in Photoshop.

Retrograde tract tracing

Retrograde tracing of the perforant pathway was performed using microinjections of 1μl Fluorogold (2%, Fluorochrome Inc., Denver, CO) delivered into the hilus of the wild type and DKI mouse dentate gyrus using a small animal stereotaxic apparatus (coordinates from Bregma -AP:1.8; DV:2.1; ML:0.75). The injected mice were between 25-30 gm in body weight. Animals were anesthetized with isofluorane, which was monitored during the surgical procedure. Surgeries were performed under aseptic techniques. After tracer injections, the injection cannula was slowly raised, and the incision on the skin was closed using bioglue (3M Vetbond, St. Paul,

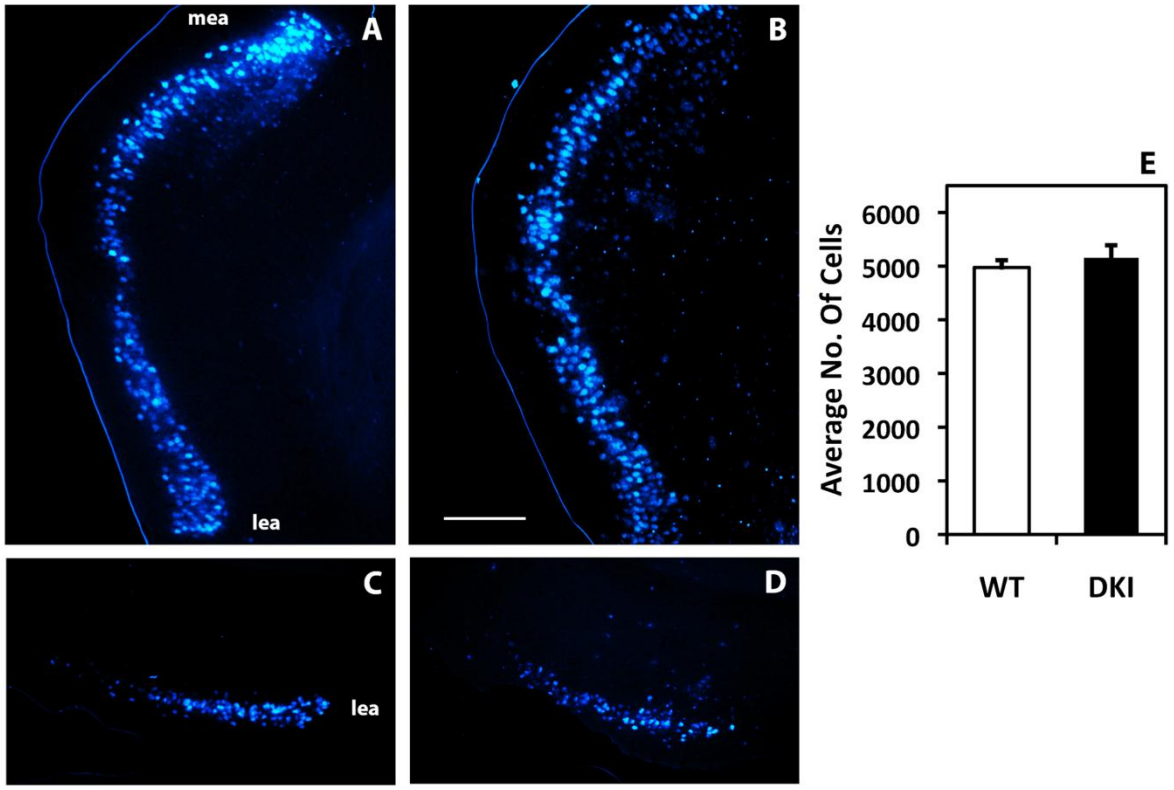

Figure 3. Retrograde labeling of the perforant pathway to evaluate neuronal loss, axonal atrophy and terminal degeneration in the aged DKI mouse. (A-D) Fluorogold accumulation is depicted in the perforant pathway neurons of origin in layer II of the dorsal entorhinal cortex (A-wild type, B-DKI) and ventral entorhinal cortex (C-wild type, D-DKI); E-Quantitative analysis of the number of retrogradely labeled neurons in entorhinal layer II at 24-27 months of age (n=8/group); mea-medial entorhinal area; lea-lateral entorhinal area. Scale bar = 500 μm.

MN). Mice were administered appropriate analgesics and monitored every day after surgery. After 10-day survival the mice were anesthetized, perfused and prepared for histology as described above.

Quantitative Analyses

The numbers of fluorogold-positive neurons in the layer II of entorhinal cortex were quantified using the NIS Elements software and binary intensity thresholding. Every 9th section was analyzed and the number of labeled neurons obtained was multiplied by the number of series to derive the total number of neurons per entorhinal cortex for each mouse. A region of interest was drawn manually that included only the layer II neurons of the entorhinal cortex. Care was taken to exclude piriform cortex, angular insular cortex, parasubiculum and other regions adjacent to the entorhinal cortex, based on well-defined anatomical landmarks (32). Cell numbers were counted in sections extending from the ventral (-5.04 from Bregma) to dorsal extremes (-2.04 from Bregma) of the entorhinal cortex, and included the entire caudal, medial and lateral entorhinal areas. The images were processed, deconvolved and saved as 2-D projection images before quantification. Because of the density of fluorescently labeled neuronal perikarya, fluorogold-positive cells were counted manually by an investigator blinded to the genotype.

Dentate Gyrus Volume Measurement

Ventral dentate gyrus volumes were determined for the two genotypes from reelin-immunostained horizontal sections using NIS-Elements quantitation software. A region of interest was drawn around the lateral and medial edges of the dentate gyrus enclosing both blades and extending anteriorly to the rostral tip of the granule

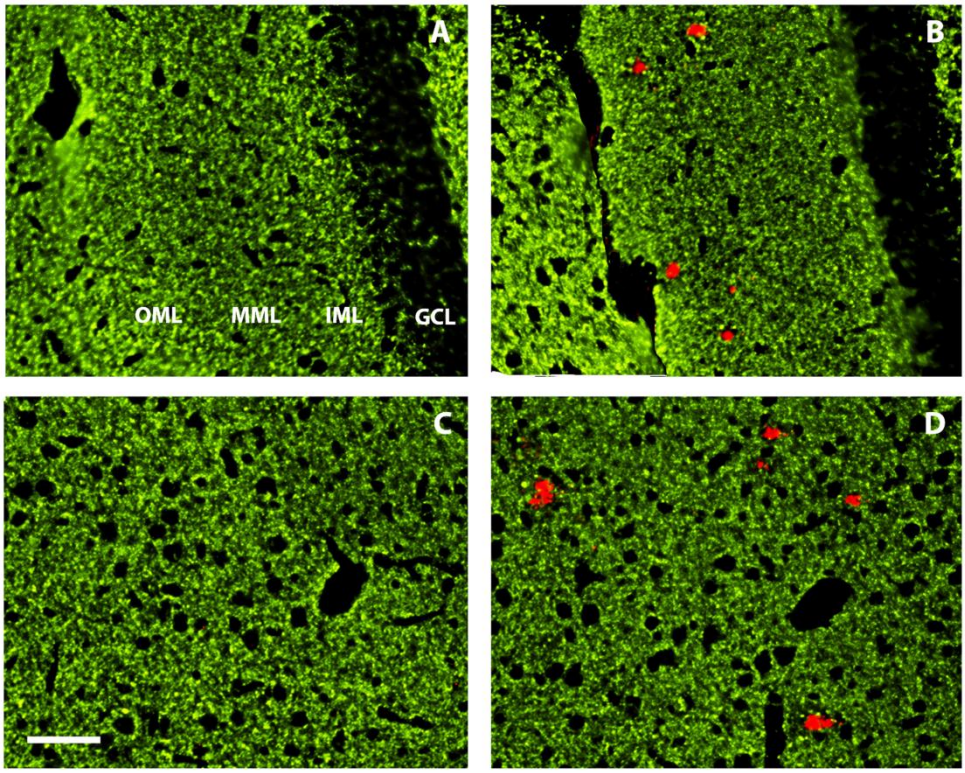

Figure 4. Lack of generalized synapse loss in the 24-27 month old DKI mouse. Representative photomicrographs of the perforant pathway terminal field in the dentate gyrus molecular layer (A,B) and also the somatosensory cortex (C,D) double labeled for the nerve terminal marker synaptophysin (green) and amyloid Aβ (red). Wild type mouse (A,C); DKI mouse (B,D). Note that the dense carpets of synaptophysin-positive nerve terminals do not differ appreciably between the two genotypes, except for the circumscribed depletion of synaptophysin staining within amyloid deposits of the aged DKI mouse. OML-outer molecular layer; MML-middle molecular layer; IML-inner molecular layer; GCL-granule cell layer. Scale bar = 50 μm.

cell layers. Every 9th section was analyzed. Volume was determined by summing the areas of each region of interest and multiplying by the number of sections between the first appearance of the two blades of dentate gyrus at its ventral border (-4.72mm from Bregma) extending dorsally to where the fibers from fimbria stop entering the caudate nucleus (-2.68mm from Bregma).

Statistical Analyses

The numbers of fluorogold -positive neurons and the dentate gyrus volumes across experimental groups were compared using Student's *t*-test with a priori *p* value of 0.05.

RESULTS

Robust amyloid deposition and advanced age do not induce neuronal loss in the mouse perforant pathway.

The DKI mouse model has familial Alzheimer-causing mutations knocked into the endogenous *APP* and *PS-1* genes, and the region encoding amyloid Aβ has been humanized (21-23, 25). In the model, amyloid deposits are first detected around 6 months of age in the hippocampus and neocortex, and the amyloid burden continues to increase steadily over time thereafter (9, 24, 25). In the current study, we evaluated AD type neuropathologies at the advanced age of 24-27 months.

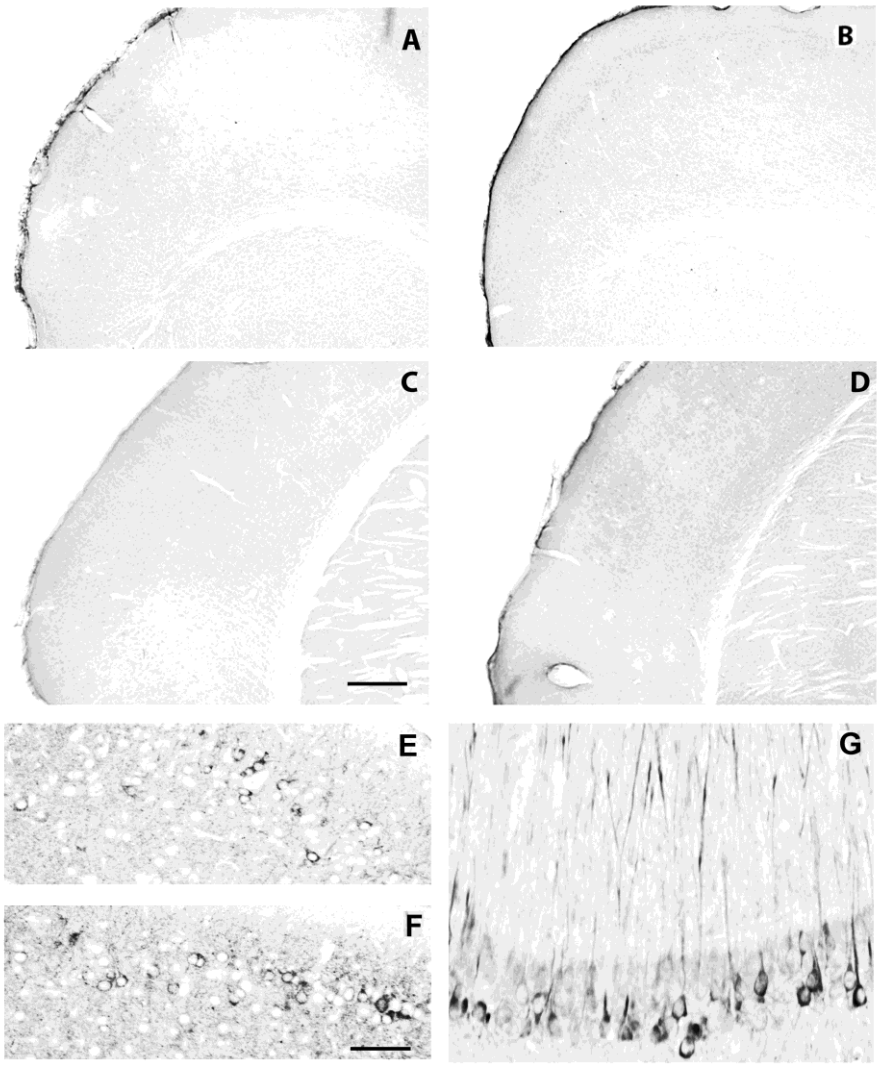

Figure 5. Hyperphosphorylated pre-tangle tau is absent from the aged DKI mouse brain. Immunoperoxidase staining using monoclonal antibody MC1 (9) in entorhinal cortex (A,B) and frontal cortex (C,D) of 24-27 month old DKI (B, D) and wild type mice (A,C). Note the complete absence of pre-tangle tau in either genotype. Scale bar = 500 μm. Positive control tissues from transgenic mouse lines expressing pathological mutant tau show robust accumulation of hyperphosphorylated tau: entorhinal (E) and frontal (F) cortex from PS19 tau transgenic mouse; area CA1 from 3xTg AD mouse (G). Scale bar = 50 μm.

Immunostaining with an antibody directed at Aβ1-28 revealed extensive deposits of amyloid of various sizes and morphologies in the molecular layer of dentate gyrus, deep layers of entorhinal cortex, and layers I-V of frontal, parietal, and temporal neocortex. Thioflavin S staining confirmed that a subset of the deposits labeled for Aβ were fibrillar core-containing plaques (Fig. 1).

The perforant pathway projects from neurons in layer II of entorhinal cortex to the hippocampal dentate gyrus and is exquisitely vulnerable to developing plaque and tangle pathologies and degeneration early in AD (14, 33, 34). Consequently, we focused on this pathway in searching for aging-dependent AD-type neuro-degeneration and neuropathology in the DKI mouse

model. The neurons of origin for the perforant pathway were labeled by immunostaining for reelin, which is preferentially expressed at high levels in these neurons in the adult mouse and human (27, 35). As shown in Fig. 2 for both ventral and dorsal aspects of entorhinal cortex, reelin expression was intense in the perikarya of entorhinal layer II neurons in 24-27 month old wild type mice, and was maintained at the same density and expression level in DKI mice (compare panels A with B and C with D). To investigate further the survival of perforant pathway neurons of origin in the aging DKI mouse, adjacent sections were immunostained for the general neuronal nuclear marker NeuN. Once again, at both ventral and dorsal levels the density of NeuN-positive neurons in entorhinal cortex layer II was indistinguishable between wild type and DKI mice. Furthermore, the densities of reelin- and NeuN-positive layer II neurons did not differ as a function of genotype for either the medial or lateral entorhinal areas, which segregate into the medial and lateral perforant pathway projections, respectively (36). These data provide evidence that the APP/PS-1 double knock-in mutations cause no appreciable loss of medial or lateral perforant pathway neurons in the aging mouse brain even in the face of an extensive and long-lasting amyloid burden in the terminal fields in the dentate gyrus. Furthermore, no other forebrain region exhibited an appreciable reduction in the density of NeuN-positive neurons in the aging DKI mouse brain (data not shown).

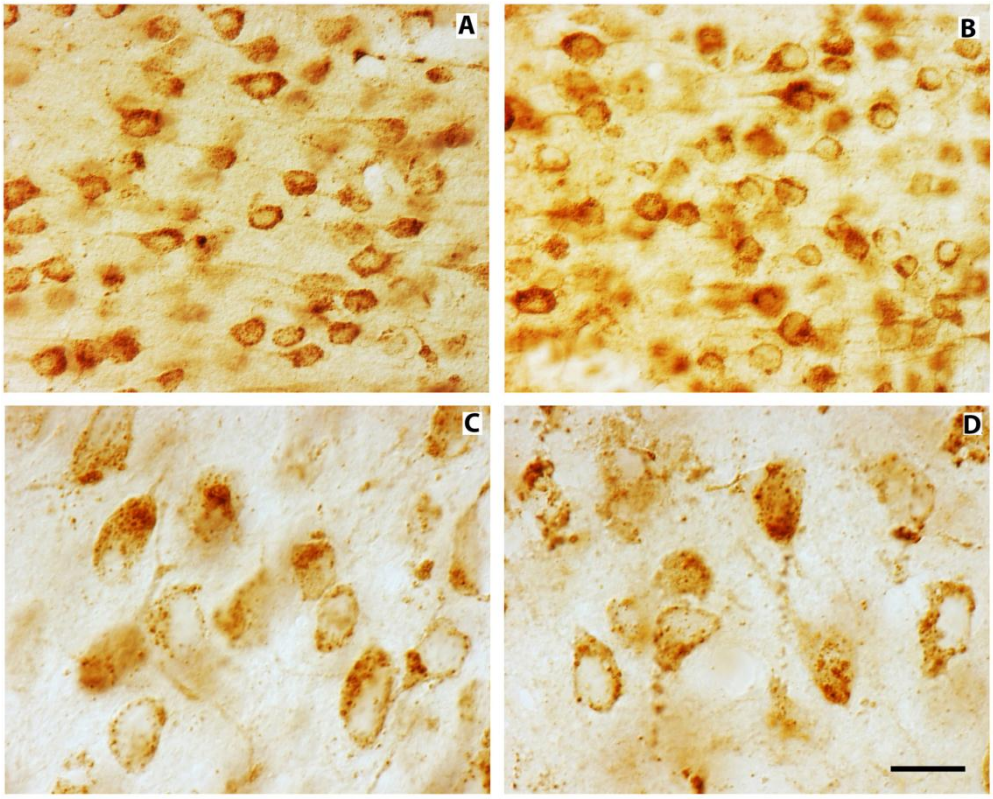

Figure 6. Evidence for lack of lysosome accumulation in the aged DKI mouse brain. Immunoperoxidase staining for cathepsin D (Yang et al., 2011) at 24-27 months of age in the frontal cortex (A,B) and subiculum (C,D) of the DKI mouse (B,D) compared to the wild type mouse (A,C). Cathepsin D immunoreactivity is confined to small perikaryal lysosomes and lysosome-related vacuoles, and is not altered appreciably in the aged DKI mouse brain. Scale bar = 50 μm.

Perforant pathway integrity is maintained with robust amyloid deposition and advanced age

In the absence of evidence for frank neuronal loss, we evaluated other features of perforant pathway integrity in aging wild type and DKI mice using retrograde tracing with Fluorogold. This method could uncover any nerve terminal loss or axonal atrophy that might accompany amyloid deposition and advanced age even in the absence of frank neuronal loss. Ten days after the tracer was microinjected into the perforant pathway terminal fields in the dentate gyrus, layer II neurons in entorhinal cortex selectively exhibited strong Fluorogold staining. The number of retrogradely labeled neurons was unaltered in the 24-27 month old DKI mouse throughout the dorso-ventral extent of the entorhinal cortex (Fig. 3 [B], [D]) as compared to wild type controls (Fig. 3 [A], [C]). Quantitative analysis confirmed that the number of retrogradely labeled perforant pathway neurons in the medial and lateral entorhinal areas did not differ between the two genotypes (Fig. 3 [E]). Additional qualitative inspection of the medial and lateral entorhinal areas at both dorsal and ventral aspects revealed no evidence for localized neuronal atrophy within any entorhinal subfield. Finally, volumetric analysis of the ventral dentate gyrus, a target for the perforant pathway, also showed no evidence for atrophy in the aging DKI mouse (1.18 +/- 0.01 mm^3) compared to the wild type mouse (1.20 +/- 0.02 mm^3).

Prolonged amyloid deposition and advanced age do not induce generalized synapse loss

Extensive loss of synapses is a cardinal feature of several neocortical and limbic regions in AD, but the degree to which transgenic mouse models recapitulate the synapse loss has been controversial, with most models failing to exhibit widespread synapse loss (37). For the DKI mouse at 14 months of age, we reported previously that synapse loss was confined to circumscribed amyloid plaques (9). Here, to evaluate the extent of synapse loss in the 24-27 month old DKI mouse brain, we used immunostaining for the synaptic vesicle protein and nerve terminal marker synaptophysin. In the perforant pathway terminal fields in the outer two-thirds of the dentate molecular layer, synaptophysin labeling was concentrated in a dense carpet of small puncta, as expected for its localization to synapses (Fig. 4 in green). There was no appreciable difference in the density of labeled nerve terminals between wild type and DKI mice. As reported previously for 14 month old mice, at 24-27 months of age the only interruptions to the dense distribution of synapses were microvessels and focal amyloid deposits (Fig. 4; amyloid deposits in red). Similarly, no cortical region exhibited any generalized synapse loss beyond the nerve terminal depletion occurring within circumscribed amyloid plaques.

Absence of tau pre-tangles in the DKI mouse brain at advanced age

The perforant pathway projection neurons in entorhinal layer II are thought to be the first to develop tau-containing neurofibrillary tangles in AD patients (34). Consequently, we searched for tangle pathology in this pathway of the DKI mouse by immunostaining with antibody MC-1. This monoclonal reacts with a pathological conformational form of tau, and labels non-paired helical filament pre-tangles in the Alzheimer brain as well as certain mouse transgenic models of tauopathy (29). Even at 24-27 months of age and in the face of over 18 months of cerebral amyloid deposition, no accumulation of MC-1 positive hyperphosphorylated tau into pre-tangles was observed in either the entorhinal (Fig. 5 [A], [B]) or frontal cortex (Fig. 5 [C], [D]) of either the wild type or DKI mouse. To confirm that our MC-1 immunostaining method was capable of detecting pre-tangle pathology in the mouse, we examined brain and spinal cord sections derived from the PS19 and 3xTg AD mouse lines. Both models express an FTLD-linked P301 mutant human tau transgene at high levels and reportedly develop extensive tauopathy in stereotypical regions of the central nervous system as adults (6, 38). Consistent with previous reports, tau pre-tangles labeled with MC-1 were readily observed within neurons of the PS19 entorhinal and frontal cortex (Fig. 5 [E], [F]) and 3xTg AD hippocampal CA1 sector (Fig. 5 [G]). Therefore, a method confirmed to label the tauopathy of two different transgenic mouse lines failed to detect any tau pathology in the 24-27 month old DKI mouse brain. Essentially identical results were obtained with TG-3, a second monoclonal that selectively labels hyperphosphorylated pre-tangle tau (data not shown).

Lack of accumulation of lysosomes in the face of robust amyloid deposition and advanced age

Surviving neurons in vulnerable regions of the AD brain exhibit massive accumulation of lysosomes and/or autophagolysosomes, as evidenced by their intense labeling for the protease cathepsin D and several other lysosomal hydrolases (31, 39). Therefore, we searched in the DKI mouse brain for aberrant accumulation of lysosomes and lysosome-related autophagic vacuoles by immunostaining for cathepsin D. The antibody used for these experiments reacts with the mouse ortholog of

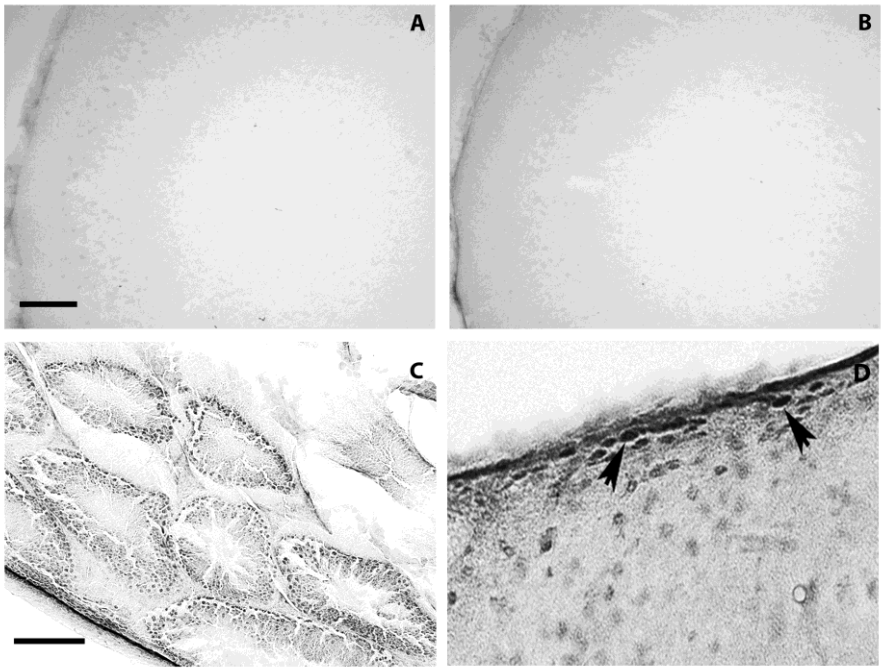

Figure 7. Advanced aged and cerebral amyloid deposition fails to induce aberrant neuronal cell cycle reentry in the mouse brain. Immunoperoxidase staining for the cell cycle marker cyclin A is undetectable in the frontal cortex of the 24-27 month old DKI (B) and wild type mouse (A); scale bar=500 μm. Positive controls for cyclin A immunostaining: proliferating cyclin A-positive cells in the seminiferous tubules from testis (C) and the subventricular zone from brain (D). In the latter, arrows depict cyclin A-immunopositive neural progenitor cells. Scale bar = 50μm.

cathepsin D and reportedly demonstrates increased accumulation of lysosomes in the frontal cortex of a mouse transgenic AD model (19). As expected of a lysosomal marker, cathepsin D staining was confined to small puncta within neuronal perikarya and was excluded from neuronal nuclei and processes. In the frontal cortex, subiculum (Fig. [6]), hippocampus, and entorhinal cortex, there was no difference between the wild type and DKI mouse in the density, staining intensity, or neuronal compartmentalization of the cathepsin D-positive puncta (compare 6A with B and C with D). Thus, robust amyloid deposition and advanced age failed to induce appreciable neuronal accumulation of cathepsin-D containing lysosomes or autophagolysosomes in the aged DKI mouse brain.

Amyloid deposition and advanced age fail to induce aberrant cell cycle reentry in neurons

An hypothesis advanced for the neurodegeneration of AD is that neurons die after aberrantly trying but failing to re-enter the cell cycle (30, 40, 41). Expression of the S phase marker cyclin A has been used as an indicator for this aberrant cell cycle re-entry in vulnerable regions of the AD brain. In 24-27 month old DKI or wild type mice, the neocortex and limbic system were completely devoid of cyclin A-positive neurons (Fig. 7). The only cyclin A-positive cells observed routinely in the aged mouse brain were clusters of neural progenitor cells in the subventricular zone (Fig. 7 [D]), and these were present regardless of genotype. As further evidence that the staining method could mark cycling cells, strong cyclin A staining was observed in the highly proliferative zone of the testicular seminiferous tubules (Fig. 7 [C]).

DISCUSSION

The major finding of this study is that in the APP/PS-1 double knock-in (DKI) mutant mouse model of AD, the combination of long-lasting cerebral amyloid deposition and advanced age of 24-27 months fails to elicit any sign

of AD-type disease progression. After more than 18 months of carrying a substantial amyloid burden, aging DKI mice show no evidence for widespread neuronal or synaptic loss, tau hyperphosphorylation, reduced reelin expression, autolysosomal accumulation, or aberrant neuronal reentry into the cell cycle, all neuropathological characteristics of vulnerable brain regions in AD (34, 39, 42-45). The DKI mouse is a unique model that mimics the genetics of the familial AD without the need for ectopic overexpression of transgenes but, as reported previously for APP transgenic models of cerebral amyloidosis (reviewed by (46, 47)), it too lacks key neuropathological features of AD. The failure of mouse models bearing Alzheimer-causing mutations in *APP*, *PS-1*, or both genes to recapitulate the full neuropathological spectrum of AD in the face of advanced age and long-lasting cerebral amyloid burden emphasizes the importance of other factors for driving the progression of AD. The results have implications for development of disease-modifying treatment strategies for the disease.

The current study focused on neuropathological and neurodegenerative changes in the entorhino-hippocampal perforant pathway, which is vital for certain forms of long-term memory (10, 11). The pathway is perhaps the earliest neural circuit in AD to develop neurofibrillary tangle and amyloid pathologies, in the neurons of origin and their terminal fields, respectively (12, 33, 34), and exhibits substantial and progressive neuronal loss beginning with the onset of mild cognitive impairment (13, 14). Similar to the AD brain, the DKI mouse develops an extensive amyloid burden in the perforant pathway terminal fields in the outer molecular layer of the dentate gyrus accompanied by neuritic dystrophy and reactive gliosis (Fig. 1; (9, 25)). Here, we investigated neuronal degeneration and atrophy of the mouse perforant pathway using four different techniques. Reelin is a selective marker for entorhinal layer II neurons of origin for the mouse and human perforant pathway (35), and reportedly shows dramatic reductions in the AD brain and a transgenic mouse model (45). We found no evidence for a decline in either the number of reelin-positive neuronal perikarya or the level of reelin expression in the aged DKI mouse in comparison with age-matched wild-type controls (Fig. 2 [A-D]). These findings are substantiated by staining for the neuronal nuclear marker NeuN, which also does not vary between aged wild-type and DKI mice in layer II of the entorhinal cortex (Fig. 2 [E-H]) or any other forebrain regions (data not shown). Additionally, after fluorogold microinjections into the dentate gyrus the number of retrogradely labeled perforant pathway projection neurons does not differ, providing further evidence that the circuit exhibits neither appreciable loss of neurons and synapses nor axonal atrophy (Fig. 3). Finally, labeling for the nerve terminal marker synaptophysin shows no depletion of perforant pathway synapses in the dentate molecular layer terminal fields beyond that associated with the circumscribed amyloid deposits (Fig. 4; (9)). Our findings in mice of advanced age confirm and extend studies of middle aged APP transgenic and APP/PS-1 bitransgenic lines, which develop entorhinal atrophy and degeneration only with additional genetic manipulations that in humans are not linked to familial forms of AD (6, 15, 17, 18).

What might account for the failure of the DKI and transgenic mouse models carrying AD-causing gene mutations even into old age to recapitulate the vulnerability of the perforant pathway? Insights to this question may lie in recent findings about the temporal progression of early pathological changes of AD. Cerebrospinal fluid biomarker profiles and neuroimaging studies of amyloid plaques have provided evidence that cerebral amyloid deposition is an early pathological process associated with an antecedent phase of AD, years before the first clinical manifestations of cognitive or behavioral problems (48-50). Given that it may take many years or even decades for AD to progress from a preclinical stage with amyloid deposition to a clinical phase, in which substantial neuronal and synapse loss underlie progressive cognitive impairment, one possibility is that the lifespan of the mouse is too short for the disease to progress in a manner analogous to its clinical stages. It has also been argued that differences in brain aging or in neuroinflammatory responses between mouse and human could play a role (51-53). Still another possibility is that amyloid deposition is not an essential step in AD pathogenesis (54), although this is contraindicated by the strong human genetic evidence linking increased production of the highly amyloidogenic Aβ42 protein relative to the Aβ40 form to the disease (55). Finally, recent studies have called attention to non-fibrillar oligomeric Aβ species as being potential neurotoxic and synaptotoxic forms of amyloid (56). The possibility cannot be excluded that, despite the extensive amyloid deposition in the DKI mouse and the presence of homozygous mutations in both APP and PS-1 that raise brain Aβ42 concentrations even prior to the onset of amyloid deposition (22), the DKI mouse brain may lack a particular toxic conformer of amyloid Aβ. These many possibilities will require further investigation.

In addition to the lack of an overt neurodegenerative phenotype, the DKI mouse at advanced age also shows no evidence for the tauopathy or aberrant neuronal cell cycle reentry that characterize vulnerable brain regions

in AD. The monoclonals we used to search for hyperphosphorylated tau are capable of detecting pre-tangles in the AD brain as well as transgenic mouse lines overexpressing a mutant form of human tau linked to frontotemporal lobar degeneration (Figure 5; (6, 29, 57)). Similarly, the cell cycle marker cyclin A is expressed at high levels in the neurogenic subventricular zone as well as the proliferative region of the testis, but is completely absent from the entorhinal cortex or any other region of the aged DKI mouse forebrain (Fig. 7). Several studies suggest that the aberrant cell cycle activation in postmitotic neurons might induce cell death in AD (30, 58, 59). A possible connection between the tau hyperphosphorylation and aberrant neuronal cell cycle reentry is that mitotic protein kinases regulating cell cycle progression also may participate in the abnormal hyperphosphorylation of tau to promote its propensity to aggregate (44). It is perhaps not surprising, then, that the aged DKI mouse model lacking an overt neurodegenerative phenotype also shows no signs of aberrant neuronal cell cycle reentry or pathological tau hyperphosphorylation.

Dysfunction of the autophagic-lysosomal pathway and hyperaccumulation of lysosomal hydrolases is another pathological hallmark of surviving neurons in brain regions vulnerable to degeneration in AD (60, 61) that appears lacking in the aged DKI mouse brain. Recent evidence has been presented that PS-1 is essential for lysosomal acidification and autophagy and that familial AD-linked mutations of PS-1 cause a marked loss of these functions, suggesting an important role for autophagic dysfunction in AD. However, in the aged DKI mouse, which is homozygous for an FAD-linked PS-1 P264L mutation, there is no detectable cathepsin D accumulation in the lysosomes and related autophagic vacuoles in any brain region (Figure 6). The lack of autophagic dysfunction is not restricted to this PS-1 mutation since, among the many mutant PS-1 expressing transgenic mouse lines, there is only a single report of a mild, regionally restricted lysosomal accumulation (62). There is also evidence that AD-causing PS-1 mutations cause a partial loss of PS-1 function that predisposes neurons to degeneration (63). However, despite the DKI mouse line expressing purely mutant and no wild type PS-1, overt neurodegeneration is not observed in any brain region even at advanced age and in the face of long-lasting cerebral amyloid deposition.

Based on the data from the DKI model coupled with transgenic mouse lines, it is now clear that amyloid deposition and advanced age are insufficient to induce the full neuropathological spectrum of AD. Since the DKI mouse is a clean model of amyloid deposition, it should be a useful experimental tool for delineating additional pathogenic factors required for driving disease progression. Further studies involving genetic and pharmacologic manipulations in the DKI model to modulate tau metabolism, autophagic function, cell cycle-related genes and kinases, and other potential pathogenic processes should help elucidate the triggering mechanisms that initiate the massive neurodegeneration and consequent cognitive and behavioral symptoms of AD. The mechanisms that drive progression of AD from its antecedent to its clinical phases beyond amyloid deposition may be important targets for novel disease-modifying treatment strategies.

ACKNOWLEDGEMENTS

Supported by NIH grant R01 AG17138 to R.S. We thank Drs. Virginia Lee and John Trojanowski for providing central nervous system tissues from transgenic mutant tau mice, Dr. Ralph Nixon for providing the antibody to mouse cathepsin D, and Dr. Peter Davies for providing monoclonal antibodies to hyperphosphorylated pre-tangle tau.

REFERENCE LIST

[1] Games D, Adams D, Alessandrini R, Barbour R, Berthelette P, Blackwell C, Carr T, Clemens J, Donaldson T, Gillespie F (1995). Alzheimer-type neuropathology in transgenic mice overexpressing V717F beta-amyloid precursor protein. Nature, 373:523-7.

[2] Lamb BT (1995). Making models for Alzheimer's disease. Nat Genet, 9:4-6.

[3] Hsiao K, Chapman P, Nilsen S, Eckman C, Harigaya Y, Younkin S, Yang F, Cole G (1996). Correlative memory deficits, Abeta elevation, and amyloid plaques in transgenic mice. Science, 274:99-102.

[4] Sturchler-Pierrat C, Abramowski D, Duke M, Wiederhold KH, Mistl C, Rothacher S, Ledermann B, Burki K, Frey P, Paganetti PA, Waridel C, Calhoun ME, Jucker M, Probst A, Staufenbiel M, Sommer B (1997). Two amyloid precursor protein transgenic mouse models with Alzheimer disease-like pathology. Proc Natl Acad Sci U S A, 94:13287-92.

[5] Holcomb L, Gordon MN, McGowan E, Yu X, Benkovic S, Jantzen P, Wright K, Saad I, Mueller R, Morgan D, Sanders S, Zehr C, O'Campo K, Hardy J, Prada CM, Eckman C, Younkin S, Hsiao K, Duff K (1998). Accelerated Alzheimer-type phenotype in transgenic mice carrying both mutant amyloid precursor protein and presenilin 1 transgenes. Nat Med, 4:97-100.

[6] Oddo S, Caccamo A, Shepherd JD, Murphy MP, Golde TE, Kayed R, Metherate R, Mattson MP, Akbari Y, LaFerla FM (2003). Triple-transgenic model of

Alzheimer's disease with plaques and tangles: intracellular Abeta and synaptic dysfunction. Neuron, 39:409-21.

[7] Stalder M, Phinney A, Probst A, Sommer B, Staufenbiel M, Jucker M (1999). Association of microglia with amyloid plaques in brains of APP23 transgenic mice. Am J Pathol, 154:1673-84.

[8] Wirths O, Bayer TA (2010). Neuron loss in transgenic mouse models of Alzheimer's disease. Int J Alzheimers Dis, *in press*.

[9] Malthankar-Phatak G, Poplawski S, Toraskar N, Siman R (2011). Combination therapy prevents amyloid-dependent and -independent structural changes. Neurobiol Aging, *in press*.

[10] Staubli U, Ivy G, Lynch G (1984). Hippocampal denervation causes rapid forgetting of olfactory information in rats. Proc Natl Acad Sci U S A, 81:5885-7.

[11] Sauvage MM, Beer Z, Ekovich M, Ho L, Eichenbaum H (2010). The caudal medial entorhinal cortex: a selective role in recollection-based recognition memory. J Neurosci, 30:15695-9.

[12] Braak H, Braak E (1990). Neurofibrillary changes confined to the entorhinal region and an abundance of cortical amyloid in cases of presenile and senile dementia. Acta Neuropathol, 80:479-86.

[13] Price JL, Ko AI, Wade MJ, Tsou SK, McKeel DW, Morris JC (2001). Neuron number in the entorhinal cortex and CA1 in preclinical Alzheimer disease. Arch Neurol, 58:1395-402.

[14] Gomez-Isla T, Price JL, McKeel DW, Jr., Morris JC, Growdon JH, Hyman BT (1996). Profound loss of layer II entorhinal cortex neurons occurs in very mild Alzheimer's disease. J Neurosci, 16:4491-500.

[15] Zhu Y, Hou H, Rezai-Zadeh K, Giunta B, Ruscin A, Gemma C, Jin J, Dragicevic N, Bradshaw P, Rasool S, Glabe CG, Ehrhart J, Bickford P, Mori T, Obregon D, Town T, Tan J (2011). CD45 deficiency drives amyloid-beta peptide oligomers and neuronal loss in Alzheimer's disease mice. J Neurosci, 31:1355-65.

[16] Kocherhans S, Madhusudan A, Doehner J, Breu KS, Nitsch RM, Fritschy JM, Knuesel I (2010). Reduced Reelin expression accelerates amyloid-beta plaque formation and tau pathology in transgenic Alzheimer's disease mice. J Neurosci, 30:9228-40.

[17] Lewis J, Dickson DW, Lin WL, Chisholm L, Corral A, Jones G, Yen SH, Sahara N, Skipper L, Yager D, Eckman C, Hardy J, Hutton M, McGowan E (2001). Enhanced neurofibrillary degeneration in transgenic mice expressing mutant tau and APP. Science, 293:1487-91.

[18] Ribe EM, Perez M, Puig B, Gich I, Lim F, Cuadrado M, Sesma T, Catena S, Sanchez B, Nieto M, Gomez-Ramos P, Moran MA, Cabodevilla F, Samaranch L, Ortiz L, Perez A, Ferrer I, Avila J, Gomez-Isla T (2005). Accelerated amyloid deposition, neurofibrillary degeneration and neuronal loss in double mutant APP/tau transgenic mice. Neurobiol Dis, 20:814-22.

[19] Yang Y, Geldmacher DS, Herrup K (2001). DNA replication precedes neuronal cell death in Alzheimer's disease. J Neurosci, 21:2661-8.

[20] Cataldo AM, Hamilton DJ, Nixon RA (1994). Lysosomal abnormalities in degenerating neurons link neuronal compromise to senile plaque development in Alzheimer disease. Brain Res, 640:68-80.

[21] Reaume AG, Howland DS, Trusko SP, Savage MJ, Lang DM, Greenberg BD, Siman R, Scott RW (1996). Enhanced amyloidogenic processing of the beta-amyloid precursor protein in gene-targeted mice bearing the Swedish familial Alzheimer's disease mutations and a "humanized" Abeta sequence. J Biol Chem, 271:23380-8.

[22] Siman R, Reaume AG, Savage MJ, Trusko S, Lin YG, Scott RW, Flood DG (2000). Presenilin-1 P264L knock-in mutation: differential effects on abeta production, amyloid deposition, and neuronal vulnerability. J Neurosci, 20:8717-26.

[23] Siman R, Flood DG, Thinakaran G, Neumar RW (2001). Endoplasmic reticulum stress-induced cysteine protease activation in cortical neurons: effect of an Alzheimer's disease-linked presenilin-1 knock-in mutation. J Biol Chem, 276:44736-43.

[24] Flood DG, Reaume AG, Dorfman KS, Lin YG, Lang DM, Trusko SP, Savage MJ, Annaert WG, De Strooper B, Siman R, Scott RW (2002). FAD mutant PS-1 gene-targeted mice: increased A beta 42 and A beta deposition without APP overproduction. Neurobiol Aging, 23:335-48.

[25] Siman R, Salidas S (2004). Gamma-secretase subunit composition and distribution in the presenilin wild-type and mutant mouse brain. Neuroscience, 129:615-28.

[26] Savage MJ, Iqbal M, Loh T, Trusko SP, Scott R, Siman R (1994). Cathepsin G: localization in human cerebral cortex and generation of amyloidogenic fragments from the beta-amyloid precursor protein. Neuroscience, 60:607-19.

[27] D'Arcangelo G, Miao GG, Chen SC, Soares HD, Morgan JI, Curran T (1995). A protein related to extracellular matrix proteins deleted in the mouse mutant reeler. Nature, 374:719-23.

[28] Mullen RJ, Buck CR, Smith AM (1992). NeuN, a neuronal specific nuclear protein in vertebrates. Development, 116:201-11.

[29] Jicha GA, Bowser R, Kazam IG, Davies P (1997). Alz-50 and MC-1, a new monoclonal antibody raised to paired helical filaments, recognize conformational epitopes on recombinant tau. J Neurosci Res, 48:128-32.

[30] Yang Y, Varvel NH, Lamb BT, Herrup K (2006). Ectopic cell cycle events link human Alzheimer's disease and amyloid precursor protein transgenic mouse models. J Neurosci, 26:775-84.

[31] Cataldo AM, Barnett JL, Berman SA, Li J, Quarless S, Bursztajn S, Lippa C, Nixon RA (1995). Gene expression and cellular content of cathepsin D in Alzheimer's disease brain: evidence for early up-regulation of the endosomal-lysosomal system. Neuron, 14:671-80.

[32] Franklin KBJ, Paxinos G. The Mouse Brain in Stereotaxic Coordinates. 3rd ed. New York NY: Academic Press; 2008.
[33] Hyman BT, Van Hoesen GW, Kromer LJ, Damasio AR (1986). Perforant pathway changes and the memory impairment of Alzheimer's disease. Ann Neurol, 20:472-81.
[34] Braak H, Braak E (1991). Neuropathological stageing of Alzheimer-related changes. Acta Neuropathol, 82:239-59.
[35] Ramos-Moreno T, Galazo MJ, Porrero C, Martinez-Cerdeno V, Clasca F (2006). Extracellular matrix molecules and synaptic plasticity: immunomapping of intracellular and secreted Reelin in the adult rat brain. Eur J Neurosci, 23:401-22.
[36] van Groen T, Kadish I, Wyss JM (2002). Species differences in the projections from the entorhinal cortex to the hippocampus. Brain Res Bull, 57:553-6.
[37] Hock BJ, Jr., Lamb BT (2001). Transgenic mouse models of Alzheimer's disease. Trends Genet, 17:S7-12.
[38] Higuchi M, Zhang B, Forman MS, Yoshiyama Y, Trojanowski JQ, Lee VM (2005). Axonal degeneration induced by targeted expression of mutant human tau in oligodendrocytes of transgenic mice that model glial tauopathies. J Neurosci, 25:9434-43.
[39] Cataldo AM, Paskevich PA, Kominami E, Nixon RA (1991). Lysosomal hydrolases of different classes are abnormally distributed in brains of patients with Alzheimer disease. Proc Natl Acad Sci U S A, 88:10998-1002.
[40] Arendt T, Holzer M, Stobe A, Gartner U, Luth HJ, Bruckner MK, Ueberham U (2000). Activated mitogenic signaling induces a process of dedifferentiation in Alzheimer's disease that eventually results in cell death. Ann N Y Acad Sci, 920:249-55.
[41] Herrup K, Arendt T (2002). Re-expression of cell cycle proteins induces neuronal cell death during Alzheimer's disease. J Alzheimers Dis, 4:243-7.
[42] Terry RD, Masliah E, Salmon DP, Butters N, DeTeresa R, Hill R, Hansen LA, Katzman R (1991). Physical basis of cognitive alterations in Alzheimer's disease: synapse loss is the major correlate of cognitive impairment. Ann Neurol, 30:572-80.
[43] Goedert M (1995). Molecular dissection of the neurofibrillary lesions of Alzheimer's disease. Arzneimittelforschung, 45:403-9.
[44] Vincent I, Zheng JH, Dickson DW, Kress Y, Davies P (1998). Mitotic phosphoepitopes precede paired helical filaments in Alzheimer's disease. Neurobiol Aging, 19:287-96.
[45] Chin J, Massaro CM, Palop JJ, Thwin MT, Yu GQ, Bien-Ly N, Bender A, Mucke L (2007). Reelin depletion in the entorhinal cortex of human amyloid precursor protein transgenic mice and humans with Alzheimer's disease. J Neurosci, 27:2727-33.
[46] Games D, Buttini M, Kobayashi D, Schenk D, Seubert P (2006). Mice as models: transgenic approaches and Alzheimer's disease. J Alzheimers Dis, 9:133-49.
[47] Ashe KH, Zahs KR (2010). Probing the biology of Alzheimer's disease in mice. Neuron, 66:631-45.
[48] Morris JC, Roe CM, Grant EA, Head D, Storandt M, Goate AM, Fagan AM, Holtzman DM, Mintun MA (2009). Pittsburgh compound B imaging and prediction of progression from cognitive normality to symptomatic Alzheimer disease. Arch Neurol, 66:1469-75.
[49] Weiner MW, Aisen PS, Jack CR, Jr., Jagust WJ, Trojanowski JQ, Shaw L, Saykin AJ, Morris JC, Cairns N, Beckett LA, Toga A, Green R, Walter S, Soares H, Snyder P, Siemers E, Potter W, Cole PE, Schmidt M (2010). The Alzheimer's disease neuroimaging initiative: progress report and future plans. Alzheimers Dement, 6:202-11.
[50] Tarawneh R, Holtzman DM (2010). Biomarkers in translational research of Alzheimer's disease. Neuropharmacology, 59:310-22.
[51] Loerch PM, Lu T, Dakin KA, Vann JM, Isaacs A, Geula C, Wang J, Pan Y, Gabuzda DH, Li C, Prolla TA, Yankner BA (2008). Evolution of the aging brain transcriptome and synaptic regulation. PLoS One, 3:e3329.
[52] Vitek MP, Snell J, Dawson H, Colton CA (1997). Modulation of nitric oxide production in human macrophages by apolipoprotein-E and amyloid-beta peptide. Biochem Biophys Res Commun, 240:391-4.
[53] Schwab C, Hosokawa M, McGeer PL (2004). Transgenic mice overexpressing amyloid beta protein are an incomplete model of Alzheimer disease. Exp Neurol, 188:52-64.
[54] Bryan KJ, Lee H, Perry G, Smith MA, Casadesus G (2009). Transgenic Mouse Models of Alzheimer's Disease: Behavioral Testing and Considerations. In Buccafusco JJ, editor. Methods of Behavior Analysis in Neuroscience. 2nd edition. Florida: CRC Press, Chapter 1.
[55] Bettens K, Sleegers K, Van Broeckhoven C (2010). Current status on Alzheimer disease molecular genetics: from past, to present, to future. Hum Mol Genet, 19:R4-R11.
[56] Wilcox KC, Lacor PN, Pitt J, Klein WL (2011). Abeta Oligomer-Induced Synapse Degeneration in Alzheimer's Disease. Cell Mol Neurobiol, *in press*.
[57] Yoshiyama Y, Higuchi M, Zhang B, Huang SM, Iwata N, Saido TC, Maeda J, Suhara T, Trojanowski JQ, Lee VM (2007). Synapse loss and microglial activation precede tangles in a P301S tauopathy mouse model. Neuron, 53:337-51.
[58] Vincent I, Jicha G, Rosado M, Dickson DW (1997). Aberrant expression of mitotic cdc2/cyclin B1 kinase in degenerating neurons of Alzheimer's disease brain. J Neurosci, 17:3588-98.
[59] Busser J, Geldmacher DS, Herrup K (1998). Ectopic cell cycle proteins predict the sites of neuronal cell death in Alzheimer's disease brain. J Neurosci, 18:2801-7.
[60] Nixon RA, Wegiel J, Kumar A, Yu WH, Peterhoff C, Cataldo A, Cuervo AM (2005). Extensive involvement of autophagy in Alzheimer disease: an immuno-electron microscopy study. J Neuropathol Exp Neurol, 64:113-22.

[61] Yu WH, Cuervo AM, Kumar A, Peterhoff CM, Schmidt SD, Lee JH, Mohan PS, Mercken M, Farmery MR, Tjernberg LO, Jiang Y, Duff K, Uchiyama Y, Naslund J, Mathews PM, Cataldo AM, Nixon RA (2005). Macroautophagy--a novel Beta-amyloid peptide-generating pathway activated in Alzheimer's disease. J Cell Biol, 171:87-98.

[62] Cataldo AM, Peterhoff CM, Schmidt SD, Terio NB, Duff K, Beard M, Mathews PM, Nixon RA (2004). Presenilin mutations in familial Alzheimer disease and transgenic mouse models accelerate neuronal lysosomal pathology. J Neuropathol Exp Neurol, 63:821-30.

[63] Shen J, Kelleher RJ, III (2007). The presenilin hypothesis of Alzheimer's disease: evidence for a loss-of-function pathogenic mechanism. Proc Natl Acad Sci U S A, 104:403-9.